2026 IEEE International Conference on Robotics and Automation (ICRA 2026)
June 1-5, 2026. Vienna, Austria

DCL-Sparse: Distributed Range-only Cooperative Localization of Multi-Robots in Sparse and Noisy Sensing Graphs

Atharva Sagale Tohid Kargar Tasooji Ramviyas Parasuraman

***Abstract*— This paper presents a novel approach to range-based distributed cooperative localization (DCL) for robot swarms in GPS-denied environments, relying solely on inter-robot range measurements, specifically addressing the limitations of current methods in noisy and sparse settings where the geometric non-rigidity of the sensing graph creates flipping (suboptimal) effects in the localization outcomes. We propose a robust multilayered localization framework (DCL-Sparse) that utilizes distributed 1-hop shadow edges (S1-Edge) to address the non-rigidity problem and improve localization convergence in sparse and noisy sensing graphs. Our approach leverages the advantages of distributed localization methods, enhancing scalability and adaptability in large robot networks. We establish theoretical conditions for the new S1-Edge that ensure solutions exist even in the presence of noise, thereby validating the effectiveness of the new shadow edge localization. Extensive simulation and real-world experiments confirm the superior performance of our method compared to state-of-the-art techniques, resulting in a reduction of up to 93% in the localization error in DCL. These experiments demonstrate substantial improvements in localization accuracy and robustness to sparse graphs. DCL-Sparse increases the localizability of large multi-robot and sensor networks, offering a powerful tool for high-performance and reliable operations in challenging large-scale environments.**

I. Introduction

Multi-robot systems (MRS) [1], [2] play a crucial role in various real-world applications, such as urban search and rescue, mining, exploration, and environmental monitoring. In scenarios like search and rescue missions in disaster-stricken areas, robots can be deployed to explore inaccessible environments, such as collapsed buildings, dense forests, or underwater cave systems, where human intervention is difficult or dangerous. Specifically, in urban search and rescue scenarios, limited infrastructure, such as the absence of GPS and reliable communication networks, makes human teleoperation impractical due to input lag and weak connectivity. Under such conditions, robot teams must rely on distributed approaches for cooperative localization, as the lack of exact coordinate information in a global frame of reference poses a major challenge [3], [4]. To overcome this challenge, the team of robots must decide on a common coordinate frame of reference and localize themselves in that new frame of reference, which will help achieve subsequent multi-robot tasks such as formation control, object manipulation, etc.

As noted in [5], [6], a generic globally rigid (GGR) graph is a subtype of graph that has been used in works such as [7] to evaluate the rigidity of the inter-robot connection for applications in distributed approaches. In [5], the authors provide a theoretical foundation for determining the rigidity of network graphs. For a unit disk graph with a sensing radius R in a unit square area, if $R > 2\sqrt{2}\sqrt{\log(n)/n}$, with n being the number of robots, then there is a very high probability that the graph is guaranteed GGR. In scenarios where the rigidity of the graph is insufficient($r < R(GGR)$), the network consensus may not converge, but may possibly remain perpetually stuck at a local minimum [8], [9], [10]. This is also possible in rigidly connected graphs due to low-edge connectivity. These issues are coined as the "flipping" phenomenon [11], where a vertex can be reflected across a face and still preserve the relative distance constraints (inter-robot range measurements) of the graph. In MRS, this scenario can occur if there is limited connectivity to preserve bandwidth or if the formation size (that is, the configuration of the robot positions) exceeds the maximum range of the robot sensors. This "flipping" can be caused by the ambiguity in the pose estimate of the neighboring robot, causing the cooperative localization estimates to converge at a local optimum, satisfying the edge constraints but not truly representing the ground truth conditions.

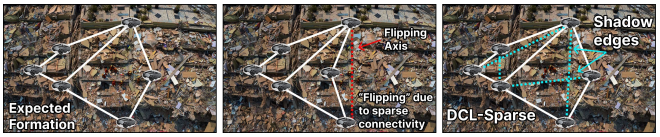

Fig. 1: Illustration of the proposed multi-robot cooperative localization in a large-scale deployment scenario. Here, the links shown in "White" are the edges of the sparsely-connected sensing and/or communication graph, in the Ground Truth frame. The second figure depicts the estimates, where the line in 'Red' represents 'flipping' of estimates due to the sparse graph setting. We add new 'shadow edges' (depicted in "Blue") from inferred information to recover the relative locations (right figure).

Another limitation in multi-robot localization is sensor noise in range measurements, which impacts the accuracy of position estimates. This noise can lead to inaccurate pose estimates, ultimately degrading precision and reliability. In practice, localization algorithms may be sensitive to these inaccuracies, potentially causing robots to converge on incorrect solutions. This can exacerbate flipping issues even in a GGR guaranteed graph, where the system may converge to a local minimum due to noisy range measurements.

Contributions: To overcome the limitations of existing methods in noisy and sparsely connected environments, we introduce a novel range-based distributed cooperative localization (DCL-Sparse) framework for robot swarms in GPS-denied settings. Unlike previous approaches, which often rely

School of Computing, University of Georgia, Athens, GA 30602, USA.
Corresponding author email: ramviyas@uga.edu

This research is supported by the Army Research Laboratory DCIST Cooperative Agreement W911NF-17-2-0181 and USDA-NIFA Cyber-Physical Systems project award no. 2024-67021-43694.

on leader selection [12] or edge connectivity manipulations through robot mobility [7], [13] and struggle with convergence in non-GGR guaranteed graph formations, our method introduces the S1-Edge approach. The S1-Edge technique addresses the rigidity challenges of sparse graphs by considering shadow (virtual) 1-hop edges, improving structural stability by utilizing the underlying inferred information. See Fig. 1 for a pictorial representation of this deployment. This framework preserves the distributed nature of the solution and offers improved scalability and adaptability for large-scale MRS. Theoretical analysis establishes bounds on the gain coefficient for shadow edges, ensuring the algorithm's stability and accuracy in the presence of noise. Our contribution is further validated through extensive simulation experiments, demonstrating significant improvements in localization accuracy and robustness over state-of-the-art.

II. Related work

In the literature, cooperative localization has been extensively studied, with various methods proposed for MRS [14], [15], [16], [8], [17], [18], [19]. Range-only sensors practical means to aid MRS operations [20]. Recent advances in range-based localization techniques have leveraged ultra-wideband (UWB) technology for inter-robot distance measurement, providing omnidirectional sensing and long-range capabilities. Several works have demonstrated the feasibility of deploying UWB-based relative localization for robot swarms in real world settings [21], [22]. In addition to UWB, other technologies such as visual-inertial odometry (VIO) [23], LiDAR-based detection [24], and radar sensing [25] have been explored for relative localization. However, despite these advances, challenges remain in ensuring accurate localization in sparse networks where robots have limited direct observations of their neighbors or anchors, leading to potential inaccuracies. In addition, the mobility of robots has been exploited in relative localization [26], [27].

The authors in [7] proposed variants of gradient-based approaches for localization in geometrically rigid formations, using stationary beacons for accurate position information. However, these methods require multiple specialized robots (or anchor nodes) and rely on a fully connected (GGR guaranteed) graph, making them less practical in sparse settings. Cao *et al.* [12] developed an algorithm in which a leader and two reference robots are elected, and trilateration is used to determine the coordinates. This method assumes all robots can communicate with reference robots and may need to re-elect a leader if outlier robots cannot communicate. Our distributed controller operates effectively in scenarios with limited connectivity, using range-only measurements to achieve localization in sparse graphs.

Oliva *et al.* [28] proposed a localization method using shadow edges to relax the global rigidity condition in unit disk graphs. They introduced an algorithm with a necessary and sufficient localizability condition, showing that shadow edge localization can succeed where trilateration fails. Their method, effective in noisy settings, localizes more nodes and achieves lower localization error compared to trilateration, particularly after recursive least squares post-processing. But, their shadow edges are centralized and not limited to 1-hop neighbors, which limits the distributed application. Similarly, in [29], the authors proposed the InferLoc localization method using an optimization-based cooperative localization mechanism that exploits Binary Flipping Graphs (BFG), which improved the localizability of a network. However, it is a centralized approach by design, suffers from high computing requirements for its optimization, and the necessity for pre-computing the BFGs of a graph limits its applicability in time-varying graphs. In contrast, our method uses a distributed implementation of shadow 1-hop edges, remedying issues with non-rigid graphs, and improving convergence and accuracy. Our approach ensures robust performance in noisy conditions and scales effectively in large networks.

Park *et al.* [22] proposed a multilateration approach for positioning UAVs using UWB ranging to address flip ambiguity caused by planar anchor configurations. Their method involves an algebraic solution, flip correction through symmetric reflection, and nonlinear optimization, collectively enhancing positioning accuracy. Their approach relies heavily on precisely known anchor locations and assumes a relatively low level of noise in the UWB ranging measurements. However, most real-world deployments involve sensor noise and dynamic obstacles that can degrade range sensor performance, leading to inaccuracies in positioning.

Moreover, these strategies generally assume ideal geometric anchor arrangements and do not account for irregular or sparse node distributions, which are often encountered in practical UAV navigation scenarios. This limitation makes their solution less robust for dynamic and complex environments where robot placement cannot always conform to a predefined configuration. Furthermore, some of these methods incur nonlinear optimization, which suffers from computational overhead, limiting the method's real-time applicability for UAVs operating in time-critical missions. Our approach addresses these shortcomings by implementing a distributed protocol without specialized nodes. This provides a scalable and efficient solution for MRS operating in GPS-denied environments. Instead of adding sensors or relying on dense sensing graphs, we introduce shadow edges—structured virtual constraints derived from existing 1-hop neighbors that exploit local geometric consistency without increasing the communication burden. This method achieves stability in extremely constrained communication environments while avoiding flipping, representing a notable advancement in enabling practical MRS applications.

III. Background and Preliminaries

Problem Statement: In this paper, we are concerned with the relative localization problem with range-only measurements z, which can be represented as follows. Let there be a set of n robots, denoted by $V = \{v_1, \ldots, v_n\}$, arranged in a fixed formation, meaning a static configuration. The positions of these robots on the Cartesian plane are given by the set $X = \{x_1, \ldots, x_n\}$, where each position is represented as x_i, indicating the coordinates of the i^{th} robot. For an expected,

time-invariant formation, the main assumption is that each robot has a range sensor that can provide readings within a limited range. Based on the unit disk sensing model, the robots form a connected sensing graph $G = (V, E)$, where the edge set E is determined by the proximity of the robots such that $E = \{(i, j) \mid \|x_i - x_j\| \leq R\}$. Here, R represents the sensing range, and the neighborhood of the robot i is defined as $N_i = \{j \in V \mid (i, j) \in E\}$, consisting of all robots within the sensing range of robot i.

Each robot is equipped with a range sensor that receives (noisy) distance measurements of its neighbors. The problem is to estimate the relative positions x_i of all robots in a common reference frame using only these inter-robot distance measurements. The following assumptions are made.

1) All nodes start with a random position estimate $\hat{x}_i(0)$.
2) For a node $i \in \{1, 2, ..., n\}$, the neighbors of i can be measured, and the node adjusts its position estimate based on this information.
3) In the graph G, only the relative distance measurements are available, and if a node i can detect its neighbor j, then j must also be able to detect i.
4) If a robot can sense its neighbor, both can communicate information. i.e., the communication range is $\geq$ the sensing range R.
5) A network of n nodes is generic globally rigid (GGR) if it is defined by a set of pairwise distance measurements $\{d_{ij}\}$ such that the configuration of the nodes is unique up to global rigid transformations (translations and rotations), and the deviation in distance measurements is minimal, meaning that the network has a minimum sensing range that ensures this rigidity.

A. Distributed Range-only Localization

Through local neighborhood communication, robots iteratively update their position estimates $\hat{x}_i$ at τ to establish a common coordinate frame of reference by sharing current estimates and range sensor readings with the neighbors using the following update rule [7]:

$$\hat{x}_i(\tau + 1) = \hat{x}_i(\tau) + \sum_{j \in N_i} \left[\alpha \Lambda_{ij}(\tau) \cdot \Big(\hat{x}_j(\tau) - \hat{x}_i(\tau) \Big) \right] \tag{1}$$

The gain for direct edges is denoted by α. The term $\Lambda_{ij}(\tau)$ represents the inconsistency at time τ between the range sensor readings $z_{ij}(\tau)$ (measurable for $(i, j) \in E$) and the current position estimates $\hat{x}_i(\tau)$ and $\hat{x}_j(\tau)$ at time τ, and is the objective being minimized in this process to solve the cooperative range-only localization problem.

$$\Lambda_{ij}(\tau) = \|\hat{x}_j(\tau) - \hat{x}_i(\tau)\|^2 - z_{ij}^2(\tau) \tag{2}$$

Previous localization approaches, such as the one described in Eq. (1), face significant challenges with incomplete sensing and the absence of direct communication between robots. These limitations can result in inaccurate or unstable localization estimates due to the reliance on direct measurements and the assumption of a fully connected network. Such assumptions are often impractical in real-world scenarios, where sparse sensing results in "flipping" problems.

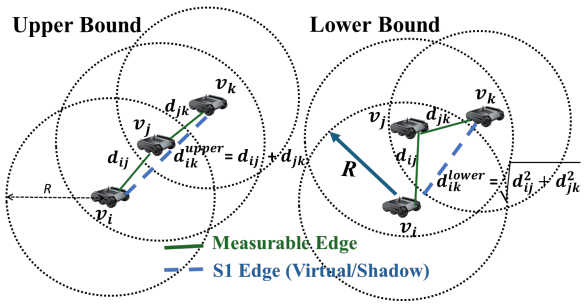

Fig. 2: Localization of robots in a network with a unit disk graph where the associated graph G is not GGR. Robots r_i, r_j, and r_k, represented by nodes v_i, v_j, and v_k. Robot r_i can detect robot r_j, but cannot detect robot r_k (i.e., node v_k is outside the dashed circle). The blue dotted line indicates a potential shadow edge that might be formed between v_i and v_k. Based on the distances d_{ij} and d_{jk}, upper and lower bounds for d_{ik} are defined.

IV. DCL-Sparse Approach

We address the limitations of the previous localization approach outlined in Eq. (1) and propose a new algorithm based on the concept of distributed shadow edges for scenarios with sparse direct sensing. A significant challenge in this process is the issue of sparsity. Without a global reference frame (GPS) the robots need to establish a reliable communication network to ensure that they can accurately localize themselves and one another. Connectivity issues can complicate the process, as some robots may be out of range or unable to communicate with others, leading to incomplete or unreliable distance information. To address this challenge, we introduce the concept of shadow edge localization. In this context, certain edges—like the one depicted by the blue dotted line in Fig. 2, are referred to as S1-Edges.

These S1-Edges help address sparsity issues (especially in non-GGR graphs) by providing additional reference points, aiding the robots in defining their local coordinate frame and achieving more accurate localization.

Definition 1: Shadow 1-hop edge (S1-Edge): In graph G, a *Shadow 1-Hop Edge* exists between a pair $(i, k) \notin E$ when robot k is indirectly connected to robot i via an intermediate node $j \in N_i$, where N_i is the set of 1-hop neighbors of i. For robots i, j, and k, where $j \in N_i$ and $k \in N_j \setminus N_i$, the distance $d_{ik} = \sqrt{d_{ij}^2 + d_{jk}^2 - 2 d_{ij} d_{jk} \cos(\delta_{ik})}$., where δ_{ik} is the angle between robots i and k connected at j. d_{ik} is bounded by $d_{ik}^{\text{upper}} \leq d_{ik} \leq d_{ik}^{\text{upper}}$:

$$\begin{aligned} &\textbf{Upper Bound:} d_{ik}^{\text{upper}} &&= d_{ij} + d_{jk}, \\ &\textbf{Lower Bound:} d_{ik}^{\text{lower}} &&= \max\left(R, \sqrt{d_{ij}^2 + d_{jk}^2}\right), \end{aligned} \tag{3}$$

where d_{ij} and d_{jk} are the Euclidean distances between consecutive robots that share an edge E. Note, the absolute bounds for d_{ik} are $R \leq d_{ik} \leq 2R$.

The S1-Edge concept enables flexible distance estimation between non-adjacent robots via intermediate nodes. The upper and lower bounds provide key insights into accuracy and feasibility. These bounds ensure reliable estimation when direct measurements are unavailable, with the upper bound

covering worst-case scenarios and the lower bound reflecting the shortest geometric distance. This approach guarantees convergence and stability in MRS, especially where maintaining communication is critical. Limiting shadow edges to 1-hop neighbors simplifies implementation and ensures scalability in distributed frameworks.

Distributed Protocol Our algorithm is defined by the following update rule, which allows distributed utilization of the S1-Edges integrated in the distributed protocol of (1).

$$\hat{x}_i(\tau+1) = \hat{x}_i(\tau) + \sum_{j\in N_i}\Big[\alpha\Lambda_{ij}(\tau)\cdot\Big(\hat{x}_j(\tau)-\hat{x}_i(\tau)\Big) + \sum_{k\in N_j/N_i}\beta S_{ik}(\tau)\Lambda_{ik}(\tau)\Big(\hat{x}_k(\tau)-\hat{x}_i(\tau)\Big)\Big], \quad (4)$$

The set of shadow S1-Edges represented as $k \in N_j \setminus N_i$, representing shadow edges that are not in the direct neighborhood set N_i of robot i and S_{ik} represents the virtual interaction between robot i and robot k (i.e., $k \notin N_i$ *if* $|x_i - x_k| > R$). Note that $S_{ik}(\tau) = 1$ if the robot i and robot k are within the range R of each other as per the current estimate $\hat{x}(\tau)$ (but they are not in reality); otherwise, it is set to zero. The gain for shadow edges is denoted by β.

Note that $\Lambda_{ik}(\tau)$ is not directly available as z_{ik} is not measurable per the sensing graph G since $(i,k) \notin E$. However, we leverage the knowledge of the S1-Edge bounds (3) we established earlier to obtain an estimate $\hat{z}_{ik}$ of the virtual edge (i,k) by considering the bounds of d_{ik} using the range measurements of (i,j) and $(j,k) \in E$, which are available or shareable in 1-hop (distributed) manner per G. The $\hat{z}_{ik}$ is calculated as

$$\hat{z}_{ik}^{upper} = (z_{ij} + z_{jk}); \quad \hat{z}_{ik}^{lower} = max(R, \sqrt{z_{ij}^2 + z_{jk}^2}) \quad (5)$$

Now, to use appropriate $\hat{z}_{ik}$, we note the fact that the objective for the DCL problem (1) and the extended DCL with S1-Edges (4) is to minimize the inconsistencies (2) for all edges (direct and shadows). Therefore, we obtain the minimum of the bounds that reduces the inconsistency with the current estimates, as given by

$$\hat{z}_{ik} = \underset{\hat{z}_{ik}=\{\hat{z}_{ik}^{upper},\hat{z}_{ik}^{lower}\}}{\arg\min} (|\|\hat{x}_i(\tau) - \hat{x}_k(\tau)\|^2 - \hat{z}_{ik}^2(\tau)|) \quad (6)$$

Accordingly, we use $\Lambda_{ik}(\tau) = \|\hat{x}_i(\tau) - \hat{x}_k(\tau)\|^2 - \hat{z}_{ik}^2(\tau)$. Here, the information about $\hat{x}_k(\tau)$ is communicated to the node i by its 1-hop neighbor node j to realize the algorithm as a distributed implementation. The S1-Edge term $\sum_{k\in N_j/N_i}\beta S_{ik}\Lambda_{ik}(\hat{x}_k - \hat{x}_i)$ is essential for improving localization performance by leveraging additional virtual connections, thus enhancing estimate accuracy in sparse and poorly connected graphs. In other words, the S1-Edge term significantly compensates for the lack of direct measurements by incorporating indirect (virtual) connections. This iterative process allows robots to achieve consensus, aligning their estimates with range measurements and establishing a common reference frame for relative positioning. The whole process is summarized in the pseudocode of Alg. 1.

Algorithm 1: Distributed DCL-Sparse Localization

Initialize:
$V \leftarrow \{v_1, v_2, \ldots, v_n\} \leftarrow$ Nodes (robots)
$X = (\hat{x}_1, \hat{x}_2, \ldots, \hat{x}_n) \leftarrow$ Initial position estimates (random)
$G \leftarrow (V, E) \leftarrow$ Graph based on sensing range
$\alpha, \beta \leftarrow$ Gain factors
Main Loop:
for $\tau = 0$ ***to*** *max_iterations* **do**
Distributed protocol applied at each robot i
for *each* $i \in V$ **do**
Information Propagation of Self + 1-Hop Estimates
for $j \in N_i$ **do**
Send: $\hat{x}_i$, $(z_{ij}, \hat{x}_j)\,\forall j \in N_i$ to j
Receive: $\hat{x}_j$, $(z_{jk}, \hat{x}_k)\,\forall k \in N_j$ from j
for $j \in N_i$ **do**
$\Lambda_{ij} \leftarrow \|\hat{x}_j - \hat{x}_i\|^2 - z_{ij}^2$
$\hat{x}_i \leftarrow \hat{x}_i + \alpha\Lambda_{ij}(\hat{x}_j - \hat{x}_i)$
for $k \in N_j \setminus N_i$ **do**
if $\|\hat{x}_i - \hat{x}_k\| < R$ *and* $\exists j \in N_i \cap N_k$ **then**
$\Lambda_{ik} \leftarrow \|\hat{x}_k - \hat{x}_i\|^2 - \hat{z}_{ik}^2$
$\hat{x}_i \leftarrow \hat{x}_i + \beta S_{ik}\Lambda_{ik}(\hat{x}_k - \hat{x}_i)$

A. Theoretical Analysis

DCL-Sparse leverages the information inferred from S1-edges to achieve stability in localization despite sparse and noisy sensing graphs. We present the main results.

Lemma 1: Consider the cost

$$V(\hat{x}) = \sum_{(i,j)\in E}\phi(\|\hat{x}_i - \hat{x}_j\| - d_{ij}), \quad (7)$$

with $\phi \geq 0$ minimized uniquely at zero. If $\bar{x}$ is a strict local minimum of V not congruent to the true configuration $x^\star$, then there exists at least one edge $(i,j) \in E$ such that the estimated displacement $(\bar{x}_j - \bar{x}_i)$ is flipped with respect to the true displacement $(x_j^\star - x_i^\star)$.

Proof: Suppose, for contradiction, that all edge orientations are preserved, i.e.,

$$(\bar{x}_j - \bar{x}_i)^\top (x_j^\star - x_i^\star) > 0, \qquad \forall (i,j) \in E. \quad (8)$$

Consider the interpolation $y(t) = (1-t)\bar{x} + tx^\star$, $t \in [0,1]$. For each edge (i,j) the scalar projection

$$s_{ij}(t) = (y_j(t) - y_i(t))^\top (x_j^\star - x_i^\star) \quad (9)$$

is continuous in t and strictly positive at both $t = 0$ and $t = 1$. Hence $s_{ij}(t) > 0$ for small $t > 0$, meaning each estimated edge $(y_j(t) - y_i(t))$ moves closer to the true edge direction.

Because $\bar{x} \ncong x^\star$, at least one distance error $\|\bar{x}_j - \bar{x}_i\| - d_{ij}$ is nonzero. Moving along $y(t)$ strictly decreases at least one such error while not increasing the others. Since ϕ is minimized at zero and nondecreasing away from zero, this yields

$$V(y(t)) < V(\bar{x}) \qquad \text{for small } t > 0, \quad (10)$$

contradicting the assumption that $\bar{x}$ is a strict local minimum. Therefore, some edge must violate the orientation condition, i.e., a flip occurs. ∎

Lemma 2: Let $V'(\hat{x}) = V(\hat{x}) + \beta\sum_{(i,k)\in S}\phi(\|\hat{x}_i - \hat{x}_k\| - d_{ik})$, and let H_V and ΔH denote the Hessians of V and the S1-edge term, restricted to the nonrigid subspace. Let $\bar{x}$ be

a spurious local minimum of V with eigenvalue $\lambda_{\min} > 0$ and $\mu_{\min} = \lambda_{\min}(\Delta H(\bar{x})) < 0$. At the true solution $x^\star$, let $\lambda^\star_{\min} > 0$ and $M^\star = \|\Delta H(x^\star)\|$. If

$$\frac{\lambda_{\min}}{-\mu_{\min}} \;<\; \beta \;<\; \frac{\lambda^\star_{\min}}{M^\star}, \tag{11}$$

then $\bar{x}$ ceases to be a local minimum of V' while $x^\star$ remains stable. Consequently, the flips associated with $\bar{x}$ (Lemma 1) are eliminated, and the DCL update (4) converges toward the global solution.

Proof: The Hessian of V' satisfies $H_{V'}(\hat{x}) = H_V(\hat{x}) + \beta\Delta H(\hat{x})$. By Weyl's inequality, the smallest eigenvalue at $\bar{x}$ obeys

$$\begin{aligned}\lambda_{\min}(H_{V'}(\bar{x})) &\le \lambda_{\min}(H_V(\bar{x})) + \beta\,\lambda_{\min}(\Delta H(\bar{x})) \\ &= \lambda_{\min} + \beta\mu_{\min}.\end{aligned} \tag{12}$$

Since $\mu_{\min} < 0$, if $\beta > \lambda_{\min}/(-\mu_{\min})$ this bound is negative, so $H_{V'}(\bar{x})$ is not positive definite, and $\bar{x}$ is no longer a local minimum.

At $x^\star$, Weyl's inequality gives

$$\lambda_{\min}(H_{V'}(x^\star)) \ge \lambda^\star_{\min} - \beta\|\Delta H(x^\star)\| = \lambda^\star_{\min} - \beta M^\star. \tag{13}$$

If $\beta < \lambda^\star_{\min}/M^\star$, then $H_{V'}(x^\star) \succ 0$, so the true solution remains a strict local minimum.

The admissible interval for β is nonempty when the inequality holds. Thus, adding S1-edges with such β destabilizes spurious minima (Lemma 1), eliminating their associated flips, while preserving global stability of $x^\star$. ∎

Theorem 1: Let $G = (V, E)$ be the communication graph of a multi-robot system, where robots $r_i \in V$ update their position estimates $\hat{x}_i$ according to the update rule (4). If the graph G is connected, and the step-size parameters β satisfy:

$$0 < \beta < \frac{2 - \alpha\lambda_2(L_d)}{\lambda_2(L_s)}. \tag{14}$$

then the localization error $e_i(\tau) = \hat{x}_i(\tau) - x^*_i$ converges to zero in the noise-free case, i.e., $\lim_{t\to\infty}\|e(\tau)\| = 0$. In the presence of bounded noise η_{ij}, the error converges to a steady-state bound: $\mathbb{E}[\|e(\tau)\|^2] \le \sigma^2$, where $\eta \sim \mathcal{N}(0, \sigma^2)$ represents the Gaussian noise in the range measurements, with variance σ^2.

Proof: **Step 1: Shadow Edge Weight.** The shadow edge weight S_{ik} is formulated based on the principle that the localization confidence is inversely proportional to the total accumulated uncertainty along an indirect measurement path. Given a three-node formation $\{i, j, k\}$, where direct measurements are unavailable between i and k, the maximum indirect measurement path as follows:

$$\|z_{ik}\| \approx \|z_{ij}\| + \|z_{jk}\| + \eta_{ik}, \tag{15}$$

where $\|z_{ij}\|$ and $\|z_{jk}\|$ are Euclidean distances obtained from relative range measurements, and η_{ik} accounts for accumulated sensor noise and potential estimation errors.

By defining the shadow edge weight as the inverse of this effective range uncertainty, we obtain the desired expression.

$$S_{ik}(t) = \frac{1}{\|z_{ik}\|} = \frac{1}{\|z_{ij}\| + \|z_{jk}\| + \eta_{ik}}, \tag{16}$$

Step 2: Error Dynamics. Define the localization error:

$$e_i(\tau) = \hat{x}_i(\tau) - x^*_i. \tag{17}$$

Substituting into the update equation:

$$\begin{aligned}e_i(\tau+1) = e_i(\tau) &+ \alpha \sum_{j\in N_i} \Lambda_{ij}(\tau)(e_j(\tau) - e_i(\tau)) \\ &+ \beta \sum_{k\in N^s_i} S_{ik}(\tau)(e_k(\tau) - e_i(\tau)).\end{aligned} \tag{18}$$

Rewriting in matrix form: $e(\tau+1) = (I - \alpha L_d - \beta L_s)e(\tau)$, where L_d is the Laplacian matrix of the direct communication graph, L_s is the Laplacian matrix of the shadow-edge graph, and I is the identity matrix.

Step 3: Spectral Analysis. The Laplacian matrices L_d and L_s are symmetric and positive semi-definite. Their eigenvalues satisfy:

$$0 = \lambda_1(L_d) \le \lambda_2(L_d) \le \cdots \le \lambda_n(L_d), \tag{19}$$

$$0 = \lambda_1(L_s) \le \lambda_2(L_s) \le \cdots \le \lambda_n(L_s). \tag{20}$$

Since $\mathcal{G}$ is connected, the smallest nonzero eigenvalue of L_d, denoted as $\lambda_2(L_d)$, is strictly positive.

The combined matrix $L = \alpha L_d + \beta L_s$ remains positive semi-definite. The spectral radius of the update matrix is:

$$\rho(I - \alpha L_d - \beta L_s) = \max_i |1 - \alpha\lambda_i(L_d) - \beta\lambda_i(L_s)|. \tag{21}$$

For stability, we require $\rho(I - \alpha L_d - \beta L_s) < 1$, which implies: $-1 < 1 - \alpha\lambda_i(L_d) - \beta\lambda_i(L_s) < 1$.

Rearranging: $0 < \alpha\lambda_i(L_d) + \beta\lambda_i(L_s) < 2$.

Thus, a sufficient condition for stability is:

$$0 < \beta < \frac{2 - \alpha\lambda_2(L_d)}{\lambda_2(L_s)}. \tag{22}$$

Step 4: Convergence to Zero Error. If α, β satisfy the above bound, then the spectral radius satisfies $\rho(I - \alpha L_d - \beta L_s) < 1$. Iterating the error dynamics:

$$\|e(\tau)\| \le \rho(I - \alpha L_d - \beta L_s)\|e(\tau-1)\| \le \cdots \le \rho^t\|e(0)\|.$$

Since $\rho < 1$, we obtain: $\lim_{t\to\infty}\|e(\tau)\| = 0$.

Step 5: Convergence with Noise. If noise η_{ij} is present, the error equation becomes:

$$e(\tau+1) = (I - \alpha L_d - \beta L_s)e(\tau) + \eta(t), \tag{23}$$

where $\eta(t)$ is a disturbance term due to noise. In steady state, the error is bounded by: $\mathbb{E}[\|e(\tau)\|^2] \le \sigma^2$, where $\eta \sim \mathcal{N}(0, \sigma^2)$ represents the Gaussian noise in the range measurements. Thus, the error is bounded by σ^2. ∎

Remark 1: The proposed localization framework ensures robustness and stability by carefully bounding the gain coefficient β associated with the shadow edges. The lower bound on β prevents underutilization of shadow edge information, maintaining efficiency even in the presence of noise. Conversely, the upper bound prevents shadow edges from dominating the localization process, ensuring that direct relative distances retain significance and the system is not destabilized by excessive shadow edge corrections. The stability of

the algorithm is guaranteed by ensuring that the eigenvalues of the system matrix $I+\alpha L_d+\beta L_s$ remain within the range $(-2, 0)$, which supports convergence to true robot positions despite noisy conditions. Theorem 1. proves that adding the β term (with β satisfying our bound) strictly reduces the worst-case spectral radius, thereby ensuring monotonic decrease of the error norm and eliminating flips even under moderate noise. Noise perturbations, both in direct distance measurements and shadow edges are accounted for, and the spectral radius condition $\rho(I+\alpha L_d+\beta L_s) < 1$ ensures that deterministic error components decay over time. As long as the noise remains bounded, the algorithm maintains stable convergence, with the final error confined within the noise-defined limits. This approach effectively mitigates the impact of noise, ensuring a stable and convergent localization.

Remark 2: The proposed S-1 edge approach increases the size of the data packet exchanged between robots without adding additional edges to the communication graph (i.e., no additional communication rounds). In a distributed algorithm, each robot communicates only with its local neighbors, whose number n is much smaller than the total system size N. Consequently, the average communication cost scales with n rather than N. Even when pseudo-neighbors are incorporated, the effective neighborhood size remains limited due to the sparsity of the network. Therefore, the added data volume from S-1 edges does not significantly impact the overall communication cost, even in large-scale robot teams.

Remark 3: The spectral condition obtained from Eq. (1) guarantees contraction of the local error dynamics and hence ensures stability of a solution, but it does not guarantee that this solution is unique. When the sensing graph lacks global rigidity, multiple non-congruent embeddings (e.g., a mirrored or "flipped" configuration) can yield identical distance measurements. In such cases, the distributed update may converge to any of these equilibria depending on initialization, which explains the flipping phenomenon observed in practice. Shadow edges mitigate this issue by introducing additional virtual constraints derived from 1-hop measurements. These extra constraints reduce the nullspace of admissible displacements that preserve all measured distances, effectively removing ambiguous solutions. Moreover, by selecting shadow distances within feasible upper and lower bounds and weighting them according to path uncertainty, the algorithm is naturally biased toward the geometrically consistent realization. Thus, while spectral contraction (via appropriate step-size choice) remains necessary for convergence, the incorporation of shadow edges provides the complementary mechanism needed to ensure uniqueness and to suppress flipping in sparse communication graphs.

V. Experiments

Experiment Setup: In our experimental setup, we set up a varying number of robots in the Robotarium [30] simulation-hardware testbed, which provides remote access to the hardware multi-robot testbed. By default, robots are arranged in a formation, such as a square lattice or a random formation, bound within the coordinates of the $3m$x$3m$ testbed. The

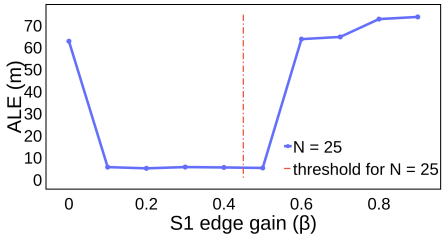

Fig. 3: (a) Confirming the bounds of S1-Edge gain (i.e., β in (4)) in the DCL-sparse approach.

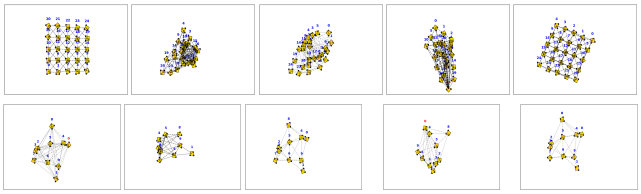

Fig. 4: Final localization results for square (top) and random (bottom) static formations for $N = 25$ and 9 respectively, using compared algorithms in $\mathbb{R}^2$. Our problem is to relative localize robots without anchor tags/reference robots; it is invariant to the orientation of the achieved formation shape.

figures shown in Fig.4 correspond to the estimate frame, which represents the hypothetical positions of the robots as they reach consensus on the shape of the formation. Due to the leaderless approach, we use the algorithm in [7] as the **baseline** distributed localization. We also implement the centralized **InferLoc** [29] solution and adapt it to a semi-distributed solution by precalculating the Binary Flipping Graphs (BFG) and using a distributed optimization strategy for the relative localization. We also implement and compare with a semi-distributed heuristic-inspired baseline variant (DCL w/ PN), where we assume a dedicated *power nodes* exist in the system that can sense and communicate with all robots. Here, strategic deployment of power nodes increases graph rigidity at the cost of scalability, but we hypothesize that adding a power node (e.g., strategically positioning a powerful UAV node) to enhance rigidity does not necessarily guarantee robust performance in sparse conditions.

Initially, we set the parameters $\beta = 0.1$, η_{kj} and η_{ij} to 0.05, the number of robots to 25, and the radius of the robot's sensing range to $R = 0.4$ (which is less than $R(GGR)$ for $N = 25$) . The connectivity graph is defined as a unit disk graph. We define the accumulation of absolute localization error (ALE) as $ALE = \sum_{i=1}^{N} \sum_{\substack{j=1 \\ j\neq i}}^{N} |\|(\mathbf{x}_i - \mathbf{x}_j\| - \|(\hat{\mathbf{x}}_i - \hat{\mathbf{x}}_j)\||$, where $\mathbf{x}$ is the position of the robots expressed in the ground truth reference frame and $\hat{\mathbf{x}}$ is the outcome of the distributed localization.

As proven in [5], for a unit disk graph with a sensing radius R in a unit square area, if $R > 2\sqrt{2}\sqrt{\log(n)/n}$, with n being the number of robots, then there is a very high probability that the graph is GGR guaranteed. We use this condition to set the R appropriately to simulate different sparsity conditions in the sensing graphs. We represent the

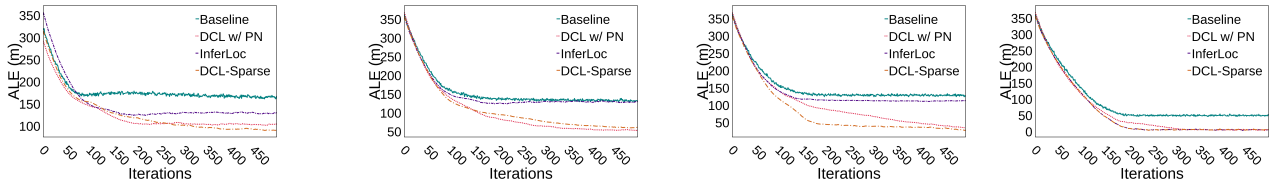

(a) R=0.4 (square, non-GGR graph) (b) R=0.4 (random, non-GGR graph) (c) R=0.67 (random, at GGR) (d) R=1.5 (random, GGR graph)

Fig. 5: Localization results with different graph sparsity with $n = 25$ and 10% sensor noise.

radius at which the GGR threshold is met as $R(GGR)$.

A. Impact of S1-Edge Gain

We examine how ALE relates to β in (4) of DCL-Sparse with $N = 25$ robots. According to Theorem 1, increasing N enhances network density and connectivity, but also introduces more noise (signal interference), which can decrease the upper bound of ALE. Additionally, more robots generally lead to closer distances between them, resulting in a higher upper bound for ALE and a greater influence of shadow edges. Despite these factors, the ALE for the DCL-Sparse algorithm remains low when the S1-Edge Gain is appropriately set within the bound, as shown in Fig. 3(a), thus validating our theoretical analysis.

B. Performance, Scalability, and Formation Analysis

In our experiments, we consider three scenarios for the rigorous analysis of distributed localization algorithms.

Qualitative Performance: We present the formation results for different localization algorithms for a square and random-shaped static initial configuration in multiple trials with a sensing radius set to vary the GGR property of the sensing graph. The results of the final ALE are presented in Table I. As shown in Fig. 4, the baseline method suffers from flipping ambiguity. InferLoc works better with fewer robots, but fails when there are more robots in the system because of the abundance of BFGs that sometimes restrict the convergence. In contrast, the DCL-Sparse method shows no flipping ambiguity as it leverages the S1-edge concept to overcome local minima conditions.

TABLE I: Final ALE after convergence in the DCL algorithms.

	Square Formation ($N = 16$)			Random Formation ($N = 25$)			Random Formation ($N = 36$)		
Approach	$r < ggr$	$r = ggr$	$r > ggr$	$r < ggr$	$r = ggr$	$r > ggr$	$r < ggr$	$r = ggr$	$r > ggr$
Baseline [7]	41.4683	40.7047	41.4683	125.2651	127.7117	51.1091	342.1098	300.0647	271.2038
Inferloc [29]	81.9532	33.7895	6.3850	116.0955	113.3078	72.6564	271.7233	193.9938	122.4565
DCL w/ PN	106.3321	38.0405	6.8638	132.2151	8.3393	6.7625	211.4830	**142.9652**	126.5745
DCL-Sparse	**3.0860**	**3.0552**	**3.0300**	**110.5973**	**7.7431**	**6.4051**	**157.7907**	144.8878	**12.422**

Impact of Graph Sparsity: We assess the evolution of ALE under different conditions of graph rigidity. Fig. 5 presents these results. Note that for radii where $0.4 <$ R(GGR) and $1.5 >$ R(GGR), the DCL-Sparse approach demonstrates superior performance compared to other methods, providing better convergence (up to 93% reduction in ALE). This is particularly notable when compared to the performance at radius 0.4 (non-GGR guaranteed sparse graph), where typical algorithms fail. The DCL-Sparse approach not only achieves superior performance at this radius but also exhibits enhanced convergence across the broader range of radii.

Impact of Robot Configuration: We assess the ALE under different ground truths (initial configurations) and radius (sensing range). As the range of robots increases, the network becomes denser, providing more connections between robots. The DCL-Sparse algorithm is designed to handle this increased connectivity efficiently. As shown in Fig. 6(a)-(b), the overall ALE for the DCL-Sparse localization algorithm is lower than for the other methods in both configurations and converges to the minimum ALE faster as the range increases.

Impact of Noise: As shown in Fig. 6(c), adding Gaussian noise to distance measurements (STD 0 to 0.3) results in only slight changes in the ALE for the proposed DCL-sparse localization algorithm, while the baseline localization method experiences significant changes (from $50m$ to $150m$). The baseline method exhibits a high sensitivity to noise, whereas the S1-edge alone performs effectively under low-noise conditions. The power node enhances sensing density and achieves a balance between low average localization error (ALE) and consistent performance; however, it remains susceptible to the noise that also propagates through the edges of the power node. Consequently, DCL-Sparse attains superior robustness relative to the baseline localization method by capitalizing on the benefits provided by the S1-edges.

Scalability: Fig. 6(d) shows that the baseline methods do not scale well as the number of robots increases, since its reliance on local neighborhood information alone results in marked performance degradation. This limitation causes the average localization error (ALE) to accumulate with increasing team size. The flipping effect is also exacerbated in larger teams, due to the greater likelihood of overlapping estimates and entrapment in local minima. In contrast, our method exploits additional inferred information through S1-edges, whose number increases proportionally with team size, thereby improving both scalability and robustness. For small systems ($N \leq 25$ robots), the Power Node baseline retains competitive performance but deteriorates beyond 36 robots. DCL-sparse algorithm demonstrates superior scalability, as it maintains lower ALE even for a larger number of robots than other methods because it can better handle network density and computational challenges that typically increase after reaching a saturation point. Finally, in Fig. 7, we demonstrate an example of the DCL-Sparse applied to an in-house real-world robot testbed (more details on this demonstration are presented in the attached video).

VI. Conclusion

This paper introduces a distributed multilayered approach for achieving distributed cooperation localization for MRS with sparse sensing graphs. It incorporates shadow edge techniques to improve robot swarm accuracy in GPS-denied

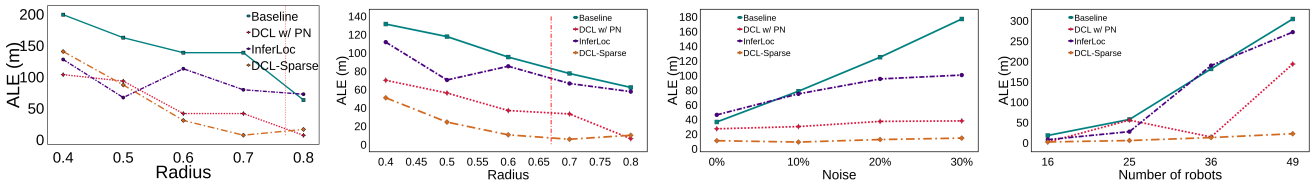

(a) Square shape formation (b) Random shape formation (c) Noise impact (d) Number of robots

Fig. 6: Impact of the robot configuration: square shape (a) and random shape (b) with n=25 and $R(GGR) \leq 0.67$, (c) sensing noise in a sparse graph with R=0.4 (non-GGR), and (d) scalability with no. of robots at R=0.67 (GGR boundary).

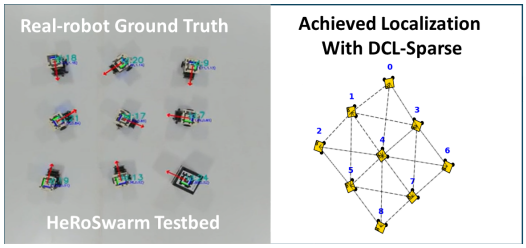

Fig. 7: Demonstration on an in-house swarm robotics testbed.

environments. The DCL-Sparse, validated through rigorous theoretical and experimental analysis, outperformed existing methods in reducing localization across different graph sparsity settings, initial robot configurations, and sensor noise levels. The algorithm scales effectively with more robots, further reducing errors.

REFERENCES

[1] L. E. Parker, "Multiple mobile robot systems," *Springer Handbook of Robotics*, pp. 921–941, 2008.

[2] Y. Rizk, M. Awad, and E. W. Tunstel, "Cooperative heterogeneous multi-robot systems: A survey," *ACM Computing Surveys (CSUR)*, vol. 52, no. 2, pp. 1–31, 2019.

[3] A. Wiktor and S. Rock, "Collaborative multi-robot localization in natural terrain*," in *2020 IEEE International Conference on Robotics and Automation (ICRA)*, 2020, pp. 4529–4535.

[4] R. R. Murphy, *Disaster robotics*. MIT press, 2017.

[5] T. Eren, O. Goldenberg, W. Whiteley, Y. R. Yang, A. S. Morse, B. D. Anderson, and P. N. Belhumeur, "Rigidity, computation, and randomization in network localization," in *IEEE INFOCOM 2004*, vol. 4. IEEE, 2004, pp. 2673–2684.

[6] R. Connelly, S. J. Gortler, and L. Theran, "Generically globally rigid graphs have generic universally rigid frameworks," *Combinatorica*, vol. 40, no. 1, pp. 1–37, 2020.

[7] G. C. Calafiore, L. Carlone, and M. Wei, "A distributed technique for localization of agent formations from relative range measurements," *IEEE Transactions on Systems, Man, and Cybernetics-Part A: Systems and Humans*, vol. 42, no. 5, pp. 1065–1076, 2012.

[8] G. Soatti, M. Nicoli, A. Matera, S. Schiaroli, and U. Spagnolini, "Weighted consensus algorithms for distributed localization in cooperative wireless networks," in *2014 11th International Symposium on Wireless Communications Systems (ISWCS)*, 2014, pp. 116–120.

[9] R. Parasuraman and B.-C. Min, "Consensus control of distributed robots using direction of arrival of wireless signals," in *Distributed Autonomous Robotic Systems: The 14th International Symposium*. Springer, 2019, pp. 17–34.

[10] T. K. Tasooji, S. Khodadadi, and H. J. Marquez, "Event-based secure consensus control for multirobot systems with cooperative localization against dos attacks," *IEEE/ASME Transactions on Mechatronics*, vol. 29, no. 1, pp. 715–729, Feb 2024.

[11] H. Ping, Y. Wang, D. Li, and T. Sun, "Flipping free conditions and their application in sparse network localization," *IEEE Transactions on Mobile Computing*, vol. 21, no. 3, pp. 986–1003, 2020.

[12] Y. Cao, M. Li, I. Švogor, S. Wei, and G. Beltrame, "Dynamic range-only localization for multi-robot systems," *IEEE access*, vol. 6, pp. 46 527–46 537, 2018.

[13] K. S. Engin and V. Isler, "Establishing fault-tolerant connectivity of mobile robot networks," *IEEE Transactions on Control of Network Systems*, vol. 8, no. 2, pp. 667–677, 2021.

[14] A. Prorok, A. Bahr, and A. Martinoli, "Low-cost collaborative localization for large-scale multi-robot systems," in *2012 IEEE International Conference on Robotics and Automation*. Ieee, 2012, pp. 4236–4241.

[15] T. H. Nguyen, T.-M. Nguyen, and L. Xie, "Flexible and resource-efficient multi-robot collaborative visual-inertial-range localization," *IEEE Robotics and Automation Letters*, vol. 7, no. 2, pp. 928–935, 2021.

[16] G. Chai, C. Lin, Z. Lin, and W. Zhang, "Consensus-based cooperative source localization of multi-agent systems with sampled range measurements," *Unmanned Systems*, vol. 2, no. 3, pp. 231–241, 2014.

[17] A. Chakraborty, K. M. Brink, and R. Sharma, "Cooperative relative localization using range measurements without a priori information," *IEEE Access*, vol. 8, pp. 205 669–205 684, 2020.

[18] Q. Guo, Y. Zhang, J. Lloret, B. Kantarci, and W. K. G. Seah, "A localization method avoiding flip ambiguities for micro-uavs with bounded distance measurement errors," *IEEE Transactions on Mobile Computing*, vol. 18, no. 8, pp. 1718–1730, Aug 2019.

[19] O. De Silva, G. K. I. Mann, and R. G. Gosine, "An ultrasonic and vision-based relative positioning sensor for multirobot localization," *IEEE Sensors Journal*, vol. 15, no. 3, pp. 1716–1726, Mar 2015.

[20] A. Quattrini Li, P. K. Penumarthi, J. Banfi, N. Basilico, J. M. O'Kane, I. Rekleitis, S. Nelakuditi, and F. Amigoni, "Multi-robot online sensing strategies for the construction of communication maps," *Autonomous Robots*, vol. 44, pp. 299–319, 2020.

[21] V. Brunacci, A. De Angelis, G. Costante, and P. Carbone, "Development and analysis of a uwb relative localization system," *IEEE Transactions on Instrumentation and Measurement*, vol. 72, no. 8505713, pp. 1–13, 2023.

[22] K. Park, J. Kang, Z. Arjmandi, M. Shahbazi, and G. Sohn, "Multilateration under flip ambiguity for uav positioning using ultrawide-band," *ISPRS Annals of the Photogrammetry, Remote Sensing and Spatial Information Sciences*, vol. V-1-2020, pp. 317–323, 2020.

[23] L. Teixeira, F. Maffra, M. Moos, and M. Chli, "Vi-rpe: Visual-inertial relative pose estimation for aerial vehicles," *IEEE Robotics and Automation Letters*, vol. 3, no. 4, pp. 2770–2777, Oct. 2018.

[24] J. Dong *et al.*, "Lidar-based cooperative relative localization," in *2023 IEEE Intelligent Vehicles Symposium (IV)*, Anchorage, AK, USA, 2023, pp. 1–8.

[25] F. de Ponte Müller, E. M. Diaz, and I. Rashdan, "Cooperative positioning and radar sensor fusion for relative localization of vehicles," in *2016 IEEE Intelligent Vehicles Symposium (IV)*, Gothenburg, Sweden, 2016, pp. 1060–1065.

[26] C. Liu, S. U. Pfeiffer, and G. C. de Croon, "Cooperative relative localization in mav swarms with ultra-wideband ranging," *arXiv preprint arXiv:2405.18234*, 2024.

[27] E. Latif and R. Parasuraman, "Dgorl: Distributed graph optimization based relative localization of multi-robot systems," in *Distributed Autonomous Robotic Systems (DARS)*, 2022, pp. 243–256.

[28] G. Oliva, S. Panzieri, F. Pascucci, and R. Setola, "Sensor networks localization: Extending trilateration via shadow edges," *IEEE Transactions on Automatic Control*, vol. 60, no. 10, Oct 2015.

[29] X. Bai, Y. Wang, H. Ping, X. Xu, D. Li, and S. Wang, "Inferloc: Hypothesis-based joint edge inference and localization in sparse sensor networks," *ACM Transactions on Sensor Networks*, vol. 20, no. 1, pp. 1–28, 2023.

[30] S. Wilson and M. Egerstedt, "The robotarium: A remotely-accessible, multi-robot testbed for control research and education," *IEEE Open Journal of Control Systems*, vol. 2, pp. 12–23, 2022.